

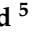



Article

Spilanthes acmella Leaves Extract for Corrosion Inhibition in Acid Medium

Akbar Ali Samsath Begum ^{1,*}, Raja Mohamed Abdul Vahith ¹, Vijay Kotra ² , Mohammed Rafi Shaik ^{3,*} , Abdelatty Abdelgawad ⁴ , Emad Mahrous Awwad ⁵ and Mujeeb Khan ^{3,*} 

¹ PG and Research Department of Chemistry, Jamal Mohamed College (Autonomous), Affiliated to Bharathidasan University, Tiruchirappalli 620001, Tamilnadu, India; abdul.vahithjmc@gmail.com

² Department of Pharmaceutical Chemistry, Faculty of Pharmacy, Queset International University Perak, Ipoh 30250, Malaysia; vijay.kotra@qiup.edu.my

³ Department of Chemistry, College of Science, King Saud University, P.O. Box 2455, Riyadh 11451, Saudi Arabia

⁴ Department of Industrial Engineering, College of Engineering, King Saud University, P.O. Box 800, Riyadh 11421, Saudi Arabia; aesayed@ksu.edu.sa

⁵ Department of Electrical Engineering, College of Engineering, King Saud University, P.O. Box 800, Riyadh 11421, Saudi Arabia; 436107822@student.ksu.edu.sa

* Correspondence: samsathshanavas@gmail.com (A.A.S.B.); mrshaik@ksu.edu.sa (M.R.S.); kmujeeb@ksu.edu.sa (M.K.); Tel.: +966-11-4670439 (M.R.S.)

Abstract: In the present study, the corrosion inhibition effect of *Spilanthes acmella* aqueous leaves extract (SA-LE) on mild steel was investigated in 1.0 M HCl solution at different temperature using weight loss, Tafel polarization, linear polarization resistance (LPR), and electrochemical impedance (EIS) measurements. Adsorption of inhibitor on the surface of the mild steel obeyed both Langmuir and Temkin adsorption isotherms. The thermodynamic and kinetic parameters were also calculated to determine the mechanism of corrosion inhibition. The inhibition efficiency was found to increase with an increase in the inhibitor concentration i.e., *Spilanthes acmella* aqueous leaves extract, however, the inhibition efficiency decreased with an increase in the temperature. The phytochemical constituents with functional groups including electronegative hetero atoms such as N, O, and S in the extract adsorbed on the metal surface are found responsible for the effective performance of the inhibitor, which was confirmed by Fourier-transform infrared spectroscopy (FT-IR) and ultraviolet-visible spectroscopic (UV-Vis) studies. Protective film formation against corrosion was confirmed by scanning electron microscopy (SEM), atomic force microscopy (AFM), and contact angle studies. The result shows that the leaves extract acts as corrosion inhibitor and is able to promote surface protection by blocking active sites on the metal.

Keywords: corrosion inhibition; *Spilanthes acmella* (SA); adsorption isotherms; LPR; EIS; Bode; contact angle



Citation: Begum, A.A.S.; Vahith, R.M.A.; Kotra, V.; Shaik, M.R.; Abdelgawad, A.; Awwad, E.M.; Khan, M. *Spilanthes acmella* Leaves Extract for Corrosion Inhibition in Acid Medium. *Coatings* **2021**, *11*, 106. <https://doi.org/10.3390/coatings11010106>

Received: 25 November 2020

Accepted: 12 January 2021

Published: 18 January 2021

Publisher's Note: MDPI stays neutral with regard to jurisdictional claims in published maps and institutional affiliations.



Copyright: © 2021 by the authors. Licensee MDPI, Basel, Switzerland. This article is an open access article distributed under the terms and conditions of the Creative Commons Attribution (CC BY) license (<https://creativecommons.org/licenses/by/4.0/>).

1. Introduction

Corrosion is typically defined as the chemical or electrochemical reaction between a material and its environment, which usually includes a metal or alloy. This process usually leads to the deterioration of the material and its properties. Mostly, the material that suffers corrosion is pure metal, but in some cases, it can also be alloys, composites, or polymers, etc. Corrosion of metals results in the deterioration of the surface of metallic structure or metal alloy in the course of their chemical, electrochemical, or biochemical interaction with the surrounding. It is an undesirable process resulting from the unwanted attack on the surface of metals or metal alloys by their environment [1]. Typically, the process of corrosion can be controlled by the use of various inhibitors which provide protection to the metal surfaces. These inhibitors delay the process of corrosion by various mechanisms. Depending on the mechanism of action, the inhibitors are classified as hydrogen evolution

poisons, adsorption type inhibitors, scavengers, vapor phase inhibitors and oxidizers. The effectiveness of an inhibitor on corrosion depends on the composition of the fluid, amount of water, and flow regime or experiment [2]. The mechanism of corrosion inhibition involves the formation of a coating film, often a passivation layer [3]. Corrosion inhibitors may prevent the electrochemical reactions by adsorbing on the surface of the metals and by forming barrier to moisture and oxygen through complexation with metal ions [4].

Among various metals, mild steel is most widely used material for many applications including reactors manufacturing, pipelines, vessels, drilling kits, energy, chemical industries and other tools. The popularity of mild steel is mainly based on its superior thermal conductivity and mechanical properties [5]. In addition, the mild steel is less expensive and easily available when compared to other materials and it also possesses long durability, superior mechanical resistance, and high toughness etc. [6]. However, steel corrosion usually ensues in acidic solution during the processes of preserving, rust-cleaning and scale-removal, and thus resulting in the need to replacement of corroded metals which leads to the massive financial losses [7]. So far, to overcome this problem, researchers have developed a variety of corrosion inhibitors which have demonstrated good inhibition efficiency, but their industrial applications have been largely inhibited due to their hazardous nature and complex developing processes [8].

Contrary to the synthetic corrosion inhibitors, plant extracts are eco-friendly and have shown several benefits including lower costs, high abundance, easy to procure etc. [9]. Researchers have started to apply the plant extracts as corrosion inhibitors way back in 1930. For instance, the pioneer application of plant extract include the use of *Chelidonium majus* extract and some other plants as corrosion inhibitors in sulfuric acid pickling baths [10]. Afterwards, the interest in using plant extracts as corrosion inhibitors has been enhanced considerably and researchers around the world reported several plant extracts [11]. According to the literature, plant extracts comprise a range of phytochemical compounds such as flavonoids, tannis, anthraquinones, amino acids, proteins, polyphenols etc. These phytochemical constituents have been deliberated as prospective corrosion inhibitors [12]. Although, plenty of plants have been tested for this purpose, the anticorrosion potential of a huge number of plants are still to be investigated. For instance, it is believed that out of ~300,000 different types of plants existed in the world, only a fraction of plants (<1%) have been investigated for their anticorrosive properties [13]. Therefore, there are huge prospects for the discovery of innovative, inexpensive, and environmental friendly corrosion inhibitors from the rich source of plants [14].

Phytomolecules such as alkaloids, flavonoids, polyphenols, amino acids and their derivatives are known to possess excellent anti-corrosive properties and have been successfully used as potential eco-friendly corrosion inhibitors, because of their low-toxicity and biodegradability [15]. For instance, Raja et al., have investigated the anti-corrosion properties of alkaloid extracts of leaves and bark of *Ochrosia oppositifolia* plant for mild steel in 1 M HCl medium [16]. Similarly, Morad et al., have studied the anti-corrosive behavior of various amino acids containing different ions on mild steel in 40% H₃PO₄ using both potentiostatic and electrochemical impedance (EIS) techniques [17]. In another study, different types of alkylamides derived from amino acids were successfully applied as anti-corrosive agents for mild steel in an aqueous solution of HCl [18]. In order to discover green corrosion inhibitors from natural products, herein, we have reported the corrosion inhibitive effect of aqueous leaves extract of *Spilanthes acmella* plant on mild steel. *Spilanthes acmella* belonging to the family Asteraceae (Genus; *Spilanthes*. Species: *S. acmella*; Botanical name: *Spilanthes Acmella*; Common name: Akarkara) is a native plant of tropical and sub-tropical regions of Asia (India) and South America [19]. This plant belongs to one of the nine plant families that are known to possess rich contents of alkaloids, flavonoids, and alkylamides as secondary metabolites [20]. These naturally occurring phytoconstituents often play an important role in various applications including plant growth-regulator functions, plant defense system, and biological functions etc., [21]. Therefore, this plant is selected based on its rich content of alkylamides which have good potential as corrosion

inhibitors. Indeed, in a recent study, plant belonging to the same family of *Spilanthes* has been used for corrosion study. Durodola et al., have used the different concentration of methanolic extract of *Spilanthes uliginosa* leaves for the investigation of corrosion of mild steel in 2.0 M HCl [22]. However, to the best of our knowledge the aqueous leaves extract of *Spilanthes acmella* plant has been rarely investigated for its anticorrosion properties.

Therefore, in this study, we have investigated the anticorrosion properties of the aqueous leaves extract of *Spilanthes acmella* plant. The anticorrosive properties of the extract was determined in 1.0 M HCl solution at various temperature using weight loss, Tafel polarization, linear polarization resistance (LPR), electrochemical impedance (EIS) (Figure 1). The thermodynamic and kinetic parameters were also calculated to determine the mechanism of corrosion inhibition. In addition, the effect of the concentration of the leaves extract on the corrosion properties was investigated by FT-IR and UV-Vis studies, while the formation of protective film was confirmed by SEM, AFM and contact angle studies confirmed protective film formation against corrosion.



Figure 1. Graphical representation of extraction and anticorrosive applications of *Spilanthes acmella* (SA) plant.

2. Materials and Methods

2.1. Materials

For the study, the leaves of SA plant are collected in the Trichy District, Tamilnadu. The plant is selected on the basis of ease of availability all over Tamilnadu. The selected plant is authenticated by the Herbarium, St. Joseph College, Trichy, Tamilnadu (India). The rolled sheets of mild steel (Fe250) containing chemical composition of sulfur (0.026%), phosphorus (0.06%), manganese (0.4%), carbon (0.1%), and iron (99.4%), is utilized for the present research work. Chemicals, such as hydrochloric acid and acetone of reagent grade are purchased from Sigma Aldrich, USA. Distilled water is obtained using a Millipore Milli-Q system, which was used in all experiments.

2.2. Methods

2.2.1. Preparation of Leaves Extract

The aqueous *Spilanthes acmella* leaves extract (SA-LE) is prepared by Soxhlet extraction (Soxhlet Medium Extractor with 250 mL flask (Thomas 4406E34, E40, E46), equipped with a heating mantle and maintained at a temperature of 60 °C). About 100 g of powdered leaves of SA is uniformly packed into thimble and extracted with 1000 mL of double distilled water (without stirrer). The process of extraction continues until the solvent in siphon tube

of the extractor becomes colorless (extraction chamber 40 mm × 115 mm (uses 25 mm thimble), condenser joint standard taper 45/50; extraction tube top joint standard taper 45/50; bottom joint standard taper 24/40 (Takes 35 × 90 mm thimble)). After the process of extraction, the extract is kept overnight for cooling and made up to 1000 mL with the same double distilled water to get 10% (*w/v*) leaves extract. Using this stock solution, different concentrations of the leaves extract solution are prepared.

2.2.2. Preparation of Mild Steel

The mild steel sheets are cut into small pieces with active surface of 5 cm × 1 cm with a thickness of 0.4 mm, which is used for the weight loss studies and 1 cm × 1 cm mild steel specimens are used for electrochemical measurements (the density of mild steel is 1 mg/cm³). The specimens are mechanically polished (polished at room temperature by using 0/0, 1/0, 2/0, 3/0, 4/0 emery papers, and kept in desiccator for further use), washed with double distilled water, degreased with acetone, and dried in hot air.

2.2.3. Selection of Medium

For this study, 1.0 M HCl is selected as the corrodent medium to analyze the inhibitive nature of SA leaves extract on mild steel corrosion. The 1.0 M HCl solution is prepared by using analytical grade reagent and double distilled water.

2.3. Corrosion Inhibition Study

2.3.1. Mass Loss Method

The mild steel specimens are immersed in stagnant solution with and without the presence of leaves extract (inhibitor) at room temperature for an immersion period of 2 h. Then, the specimens are removed, washed, and kept in desiccators. These specimens are weighed before and after immersion in the corrodent solution. The weight loss and surface coverage is calculated from the difference between the weights before and after the immersion.

$$\text{Surface coverage } (\theta) = \frac{W_0 - W_i}{W_0} \quad (1)$$

where, W_0 —weight loss without inhibitor, W_i —weight loss with inhibitor.

2.3.2. Effect of Concentrations, Temperature, and Corrosion Rate

From the stock solution, various concentrations of the extract are prepared in aqueous media. Different concentrations of the inhibitor used in the study are 2, 4, 6, 8, and 10 (*v/v*%). The effect of the temperature on the inhibitive nature is examined by weight loss method. The effect of temperature on corrosion at different concentrations of the inhibitor is studied at the temperatures 303 K, 313 K, 323 K, and 333 K for the immersion period of 2 h. The corrosion rate is calculated using the formula

$$\text{Corrosion rate } \left(\text{mg/dm}^2 \text{ day} \right) = \frac{53.5 \times W}{a \times t} \quad (2)$$

where, “W” weight loss in gram, “a” the area of the specimen in cm² and “t” time exposure in hour.

The inhibition efficiency is found using the following formula:

$$\text{Inhibition efficiency} = \frac{W_0 - W_i}{W_0} \times 100 \quad (3)$$

2.3.3. Adsorption Isotherm, Energy of Activation (E_a) and Free Energy of Adsorption ($\Delta G^\circ_{\text{ads}}$)

Adsorption isotherms provide details about the interaction between the adsorbed molecules among themselves as well as their interactions on the metal surface. The degree of surface coverage (θ) with respect to different concentrations of the inhibitor and different temperatures is determined to deduce the fittest isotherm. The experimental data are fitted

to the following two isotherms including Langmuir Isotherm—Plot of $\log(C/\theta)$ vs. $\log C$ and Temkin Isotherm—Plot of θ vs. $\log C$.

Adsorption isotherm and the mechanism of the corrosion reaction can be explained by the thermodynamic parameters. The kinetic parameters, namely activation energy (E_a) and the thermodynamic parameters such as $\Delta G^{\circ}_{\text{ads}}$, $\Delta H^{\circ}_{\text{ads}}$, $\Delta S^{\circ}_{\text{ads}}$ are calculated by the Equations given below. For the corrosion of mild steel in 1.0 M HCl, the activation energy is calculated using the Arrhenius Equation.

$$\text{Corrosion rate (CR)} = A \exp(-E_a/RT) \quad (4)$$

The logarithm on both sides of Equation gives the Equation:

$$\log \text{CR} = \log A - E_a/2.303 R \quad (5)$$

$$E_a = -2.303/R \times \text{Slope} \quad (6)$$

$\log \text{CR}$ vs. $1/T$ for the mild steel corrosion in the presence of different concentrations of aqueous leaf extract of SA gives linear straight line. From the slopes and intercepts of Arrhenius plots, the values of E_a and A were calculated.

The standard free energy of adsorption at different temperatures for various concentrations, is calculated from the Langmuir adsorption isotherm model using the equation.

$$\Delta G^{\circ}_{\text{ads}} = -2.303 RT \log (K_{\text{ads}} \times 55.55) \quad (7)$$

2.3.4. Electrochemical Methods

Potentiodynamic (Tafel) Polarization, Linear Polarization Resistance, Electrochemical Impedance, and Bode Studies

The electrochemical measurements are carried out using model CHI6608 Microcell kit Princeton electrochemical Analyzer. The mild steel specimen is machine cut into coupons of dimensions, $5 \text{ cm} \times 1 \text{ cm} \times 0.2 \text{ cm}$ and embedded in araldite (epoxy resin) leaving a 1 cm^2 surface area exposed for electrochemical measurements. A conventional three-electrode cell with mild steel as working electrode, saturated calomel electrode as reference electrode, and platinum electrode as counter electrode, is used. The potential is scanned, after a stable value of E_{corr} is reached, at a scan rate of 0.01 (V/s) from the corrosion potential in the direction of cathodic and also in the anodic direction, in the range of potential -0.80 to -0.20 V . Inhibition efficiency (I.E) is measured by the following formula:

$$\text{I.E (\%)} = \frac{I_0 - I_i}{I_0} \times 100 \quad (8)$$

where I_0 and I_i are the density values of corrosion current without and with corrosion inhibitors.

Linear polarization resistance values are measured from the slope of potential current lines, using the formula:

$$R_p = A \times \frac{dE}{Di} \quad (9)$$

Electrochemical impedance spectra are recorded over the frequency range 100 Hz to $100,000 \text{ Hz}$ and with AC signal of amplitude 0.005 V . The measurements were recorded after the electrode reaches a steady value of E_{corr} . The experiments are carried out at a constant temperature of $30 \text{ }^{\circ}\text{C}$. The charge transfer resistance R_{ct} values are obtained from the plot of Z''/ohm vs. $-Z'/\text{ohm}$ by calculating the difference in the impedance values at low and high frequencies. The C_{dl} is calculated from the relationship [23]:

$$\text{double layer capacitance } C_{\text{dl}} = \frac{1}{2\pi \times f_{\text{max}}} \times R_{\text{ct}} \quad (10)$$

where f_{max} is the frequency and R_{ct} is the charge transfer resistance.

Bode plots is obtained by the plot of $\log (Z/\text{ohm})$ and phase/deg against $\log (\text{frequency/Hz})$. From this plots, the absolute impedance $|Z|$ was calculated from the Equation $|Z| = \sqrt{(Z')^2 + (Z'')^2}$ [24] and the phase angle (Θ) is also directly noticed from the plot.

2.4. Surface Analysis

Perkin Elmer FT-IR spectrophotometer is used to record the FT-IR spectra in the range of 4000 to 400 cm^{-1} . The adsorbed phytomolecules of the leaves extract on metal surface was analyzed by FT-IR spectra [25], after it is scratched from the mild steel surface, which is immersed in 1.0 M HCl in the presence of studied leaves extract for 2 h at room temperature. To confirm the formation of metal-inhibitor complex on the surface of mild steel, PC-based double beam spectrophotometer 2202 is used. UV-Visible absorption spectrophotometric method is carried out for crude leaves extract and for the solution containing mild steel immersed in 1.0 M HCl with addition of 10% (v/v) concentration of SA extracts after 2 h immersion at room temperature [26]. SEM is used to analyze the topography of the mild steel surface after corroding in the presence and absence of the inhibitor [27]. The SEM images are taken by the JEOL MODEL JSM 6390 (15 kV). Surface morphology is determined by atomic force microscopy. After the inhibition test, the mild steel specimens were placed in vacuum desiccators, mounted on sample holder under the objective of the atomic force microscope and the 3D—images were taken from the 100 X magnified surface through operating program on computer. The surfaces of mild steel specimens were evaluated by atomic force microscopy after immersed in 1.0 M HCl solutions in the presence and absence of aqueous leaves extract of SA for two hours [28]. The adsorption nature of the inhibitor on the surface of the mild steel is verified by determining the contact angle. It is determined by goniometer using sessile drop method and the measurement is made with contact angle goniometer model 190-F1. The contact angle is measured for the surface of freshly polished mild steel as well as the mild steel after immersed in the corrosive solution in the presence and absence of 10% aqueous leaves extract of SA solution at room temperature for the immersion period of time 2 h.

3. Results and Discussion

3.1. Characterization of Aqueous Leaves Extract of SA

3.1.1. Preliminary Phytochemical Screening of the Leaves Extract

Aqueous extracts of the identified plant leaves are screened [29] for the presence of flavonoids, alkaloids, terpenoids, saponins, anthraquinones, reducing sugar, and polyphenols using standard procedure [30]. The results are given in Table 1.

Table 1. Preliminary phytochemical analysis of aqueous extract of the collected leaves.

Phytochemical Constituents	Alkaloids	Carbohydrates	Flavonoids	Tannins	Amino Acids	Terpenoids
Aqueous extract of the leaves <i>Spilanthes Acmella</i> (SA-LE)	+	—	+	+	—	—
Phytochemical Constituents	Glycosides	Steroids	Anthraquinones	Saponins	Phenols	Proteins
Aqueous extract of the leaves <i>Spilanthes Acmella</i> (SA-LE)	+	+	—	—	—	—

+: for presence; —: for absence.

3.1.2. FT-IR Spectroscopic Study of Aqueous Extract of the Leaves of SA

The FT-IR spectrum of aqueous leaf extract of SA is recorded and is given in Figure 2, the FT-IR absorption bands identified are given in Table S1, Supplementary File. A broad band at 3401 cm^{-1} is due to the stretching vibration of O–H (indicating the presence of phenolic compounds including flavonoids). The intense bands at 2924 and 2854 cm^{-1} represent the stretching vibration of aliphatic C–H (these bands could represent glycosides, like different types of sugar molecules). The sharp band at 1742 cm^{-1} is consistent with C=O stretching vibrations. The absorption peaks at 1630 cm^{-1} and 1560 cm^{-1} are attributed to the presence of C=C in aromatic ring. The band observed at 1113 cm^{-1} and 1022 cm^{-1} are probably due to the C–O stretching. The peak at 870 cm^{-1} indicates the C–Cl stretching. The CH (OOP) absorbs at 696 cm^{-1} . The FT-IR data obtained and the phyto-chemical screening results indicate the presence of the reported phyto-components in the aqueous leaf extract of SA (Table S1, Supplementary File) [31].

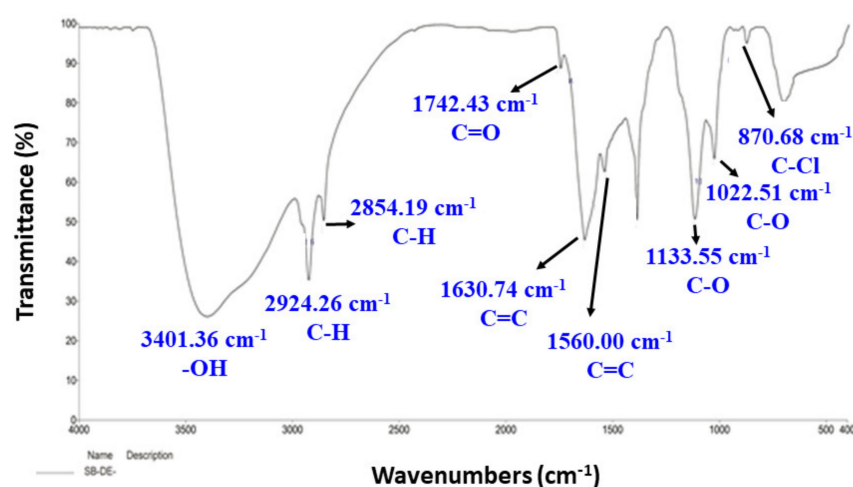


Figure 2. FT-IR spectrum of aqueous leaf extract of SA.

3.1.3. UV-Visible Absorption Spectral Studies

The phyto-chemical components present in *Spilanthes acmella* leaf extract (SA-LE) are analyzed using UV-Visible spectral studies. The absorption spectra of aqueous leaves extract of SA occurred in the 200–400 nm wavelength regions. The absorption bands (nm) noticed is mentioned in Table 2. The recorded UV-visible spectrum of aqueous SA-LE is shown (Figure 3) and the adsorption bands are indicated (Table 2). The spectrum shows major peaks at 231 and 265 nm indicating the presence of N and O atom in the phyto-chemical constituents of the SA leaf extract. The absorption maximum for the isobutylamide—NH (fatty acid) is 265 nm [32]. This is also observed in the recorded FT-IR spectra.

Table 2. UV-visible spectral absorption bands (nm) of aqueous extract SA leaves.

Inhibitor System Leaf Extract	Absorption Bands (nm)	Transitions
SA	231, 265	$\eta \rightarrow \pi^*$
		$\pi \rightarrow \pi^*$
		$\eta \rightarrow \sigma^*$

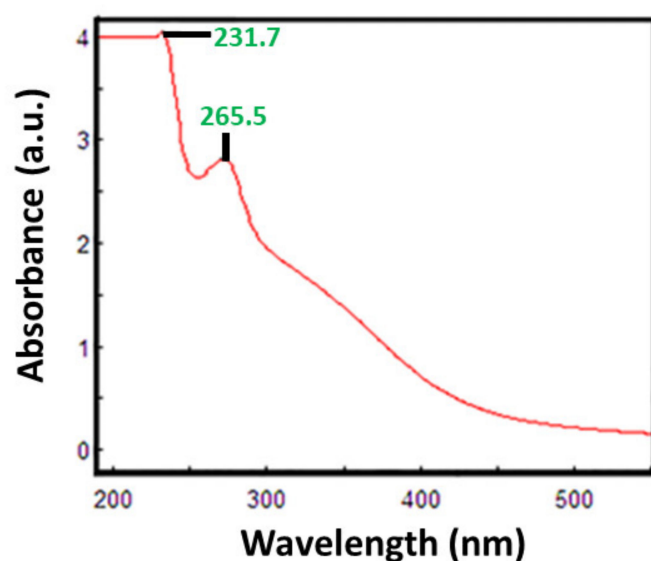


Figure 3. UV-Visible spectrum of aqueous SA-LE. Note: high peak and plateau in the spectrum could be due to the high concentration of the sample (un-diluted).

3.2. Weight Loss Method

Among many experimental methods available to determine the percentage inhibition efficiency and corrosion rate, weight loss method is the simplest and frequently used. In this study, the experiments were carried out by varying the concentrations of the inhibitor. This study is also carried out at different temperatures and the immersion period is fixed at 2 h. The weight loss calculated, in grams, is the difference between the weight of metal coupon before and after immersion in corrosive solution. The results obtained are discussed to know the effect of concentration and temperature.

3.2.1. Effect of Concentration of Leaves Extract on Corrosion Inhibition

The inhibition efficiency and the corrosion rate values for all the studied inhibitors and the blank system are determined and given in Table 3. The corrosion rate decreases and the inhibition efficiency increases with the increase in the concentration of extract for all inhibitors, and the concentration range is 2% to 10% for 2 h immersion of the metal coupon in corrosive solution at room temperature. The inhibition efficiency increases because of the inhibitor molecules present in the extract getting adsorbed on the metal surface [33]. The maximum inhibition efficiency and the lower corrosion rate are found at high concentration (10% v/v) for all inhibitors. With further increase in inhibitor concentration above 10%, the inhibition efficiency and corrosion rate almost remained constant. So the 10% is the optimum concentration of the leaves extract to achieve high activity [34].

Table 3. Inhibition efficiency of aqueous leaves extract of SA on the corrosion of mild steel in 1.0 M HCl at room temperature (303 K).

Inhibitors	Concentration of Inhibitor (% v/v)	Corrosion Rate (mg/dm ² Day)	Inhibition Efficiency (%)
SA	Blank	615	—
	2	219	64.34
	4	176	71.30
	6	123	80.00
	8	096	84.34
	10	42	93.04

3.2.2. Effect of Temperatures on the Anti-Corrosion Activity of Spilanthes Acmella Leaves SA-LE

In this case, the corrosion efficiency and corrosion rate is determined for all the inhibitor systems from 2–10% (v/v) with temperatures ranging from 303–333 K. The data of inhibition efficiency and the corrosion rate of each extract are mentioned in Table 4. The efficiency decreases from 93 to 64% and the corrosion rate increases from 42 to 219 with the rise in temperature from 303–333 K in 1.0 M HCl at the higher concentration (10%) for SA-LE. Also the same trend is obtained for other inhibitor system (Table 4). The effect of temperature increased with increasing inhibitor concentration on the dissolution of mild steel, and the partial desorption of extract from inhibitor from the surface of the metal also increases [35].

Table 4. Inhibition efficiency of SA-LE on the corrosion of mild steel in 1.0 M HCl at different temperatures.

Temperature (K)	Concentration of Inhibitor (% v/v)	Corrosion Rate (mg/dm ² Day)	Inhibition Efficiency (%)
303	Blank	615	—
	2	219	64.34
	4	176	71.30
	6	123	80.00
	8	96	84.34
	10	42	93.04
313	Blank	979	—
	2	379	61.20
	4	342	65.02
	6	310	68.30
	8	230	76.50
	10	187	80.87
323	Blank	1181	—
	2	535	52.15
	4	518	53.58
	6	470	57.89
	8	379	66.02
	10	294	73.68
333	Blank	1251	—
	2	690	44.87
	4	668	46.58
	6	577	53.84
	8	486	61.11
	10	428	65.81

3.3. Adsorption Isotherm

An adsorption isotherm gives the direct relationship between the corrosion inhibition efficiency with the degree of surface coverage at constant temperature for different concentrations of inhibitor solutions. The adsorption isotherm provides the basic information about the nature of interaction between the mild steel surface and inhibitor molecular constituents [36]. Adsorption of the corrosion inhibitor molecules occurs on the mild steel surface by the displacement of molecule of water adsorbed on the metal surface. Also, the adsorption depends on the temperature, chemical composition, and concentration of inhibitor and the electrochemical potential at the metal—solution interface [37].

There are several isotherms proposed to account for the adsorption of the corrosion inhibitor molecules on the surface of metal. From the isotherm, the linear relationship between θ and concentration of inhibitor can be found. In this study, the changes in the θ , and thereby the change in the efficiency of inhibitor is determined by using different isotherms model.

3.3.1. Langmuir Adsorption Isotherm

The degree of surface coverage (θ) for different concentrations of inhibitor (2%, 4%, 6%, 8%, and 10% (v/v)) at different temperatures (303 K, 313 K, 323 K, and 333 K) was found from the weight loss method. According to Langmuir isotherm, the following Equation relates the surface coverage (θ) and the inhibitor concentration, C:

$$\frac{C}{\theta} = \frac{1}{K_{\text{ads}}} + C \quad (11)$$

The plots of Langmuir adsorption isotherm, C/θ vs. C at different temperatures is shown in (Figure 4) for all the studied inhibitors at different temperatures.

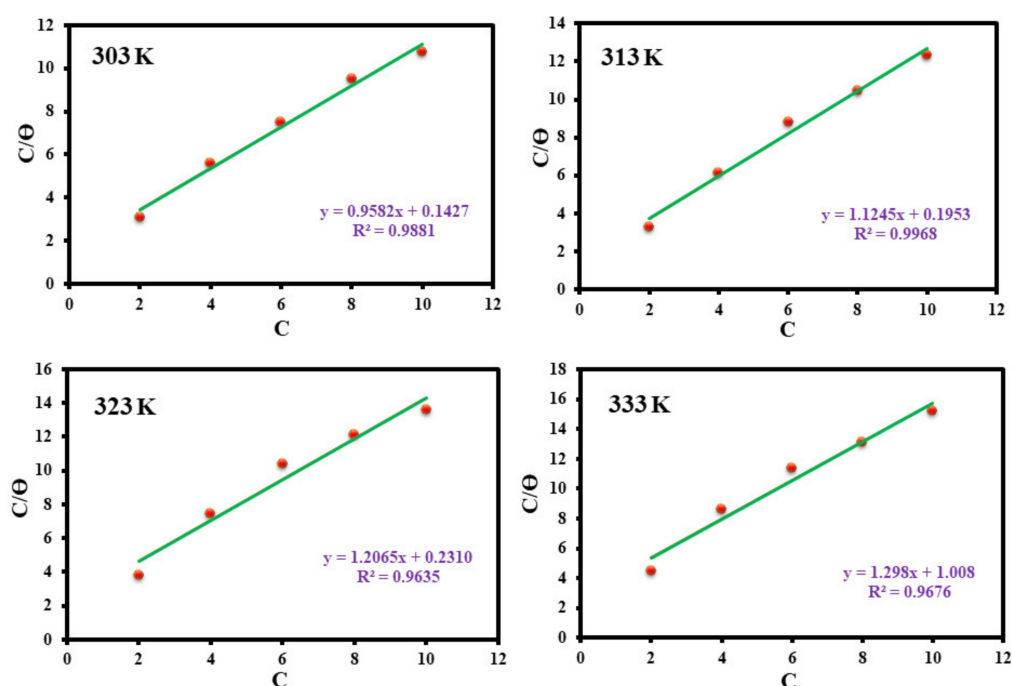


Figure 4. Langmuir adsorption isotherm for the inhibition effect of aqueous leaves extract of SA on mild steel corrosion in 1.0 M HCl at different temperatures.

The values of adsorption parameters obtained from Langmuir adsorption isotherm, including ΔG_{ads}^0 , R^2 , slope, intercept of each studied inhibitor system on mild steel surface are enlisted in Table 5. The negative value of ΔG_{ads}^0 ensures the spontaneity of the adsorption process and the stability of the adsorbed layer on the steel surface. The ΔG_{ads}^0 is calculated from the Equation:

$$\Delta G_{\text{ads}}^0 = -2.303 RT \log (K_{\text{ads}} \times 55.55) \quad (12)$$

Table 5. Adsorption parameters obtained from Langmuir adsorption isotherm for the corrosion inhibitive effect of aqueous leaf extracts of SA on the corrosion of mild steel in 1.0 M HCl.

Inhibitor System	Temperature, K	R ²	Slope	Intercept	K _{ads}	−ΔG _{ads} ⁰
SA	303	0.9981	0.9582	0.1427	7.007	15.027
	313	0.9968	1.1245	0.1953	5.120	14.706
	323	0.9635	1.2065	0.2310	4.329	14.725
	333	0.9676	1.298	1.0080	0.992	11.102

The inhibitor molecules adsorbed on the anodic and cathodic sites of the metal surface interact by mutual repulsion (or) attraction [38]. The comparison of R^2 values obtained

from Langmuir adsorption isotherm, at various temperatures shows that the isotherm fits better at 303 K than the other higher temperatures and it has been reported by many researchers [39]. The R^2 values are greater than 0.9 showing that the Langmuir plots are linear. The K_{ads} values are high at 303 K for every inhibitor and decrease with the increasing temperatures, indicating that the inhibitor is more strongly adsorbed on the metal surface at low temperature than at higher temperatures [40].

3.3.2. Temkin Adsorption Isotherm

The Temkin adsorption isotherm is based on the assumption of uniform distribution of the inhibitor (monolayer) on the metal surface. The adsorption energy linearly decreases with the increase of surface coverage values (θ). The values of surface coverage θ , at various concentrations of each inhibitor in 1.0 M HCl solution, obtained from mass loss measurements, were fitted to the Temkin adsorption isotherm shown below

$$\exp(-2\alpha\theta) = K_{ads} \cdot C \quad (13)$$

$$\theta = -\frac{2.303 \log K_{ads}}{2a} - \frac{2.303 \log C}{2a} \quad (14)$$

where, “a” denotes the lateral molecular interaction parameter. The adsorption of organic molecules at a metal-solution interface is a quasi-substitutional process between the inhibitor molecule (in aqueous solution) and water molecule (on the metal surface) [41].



where, X is the size parameter and it represents the number of adsorbed water molecules replaced by the given adsorbate (inhibitor molecule). The plot of θ vs. $\log C$ for the mild steel in 1.0 M HCl in the presence and in the absence of plant extract inhibitors SA are given in Figure 5 for various temperatures.

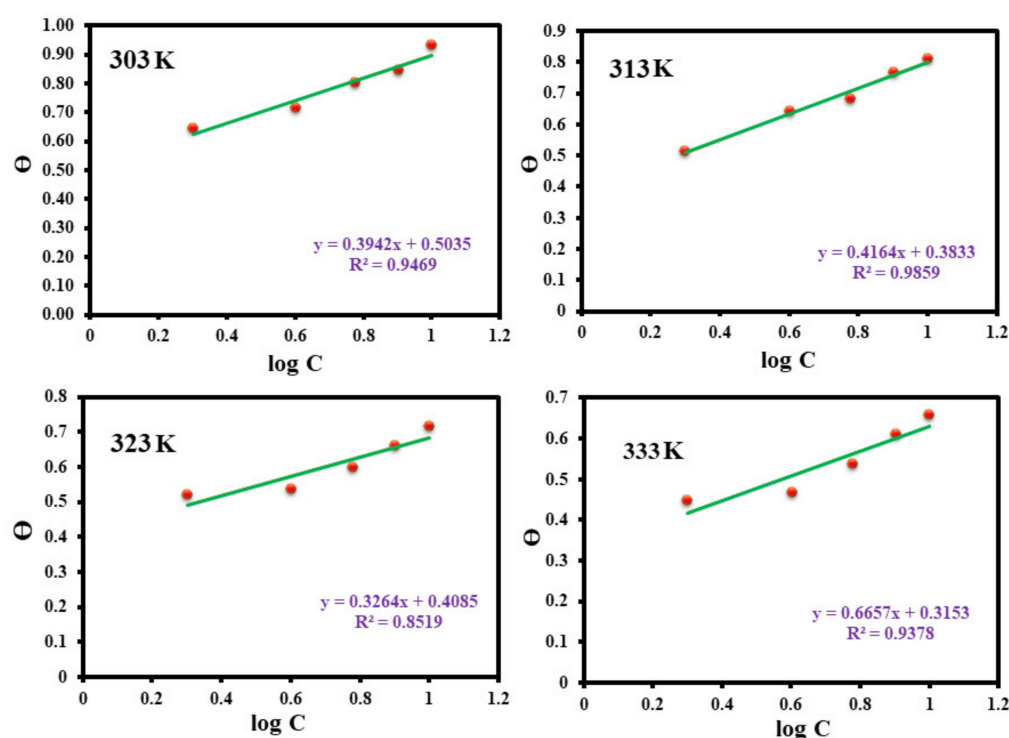


Figure 5. Temkin adsorption isotherm for the inhibition effect of aqueous leaf extract of SA on mild steel corrosion in 1.0 M HCl at different temperatures.

The values of intercept, slope, a , K_{ads} and ΔG^0_{ads} are calculated from Temkin isotherm plots, which are shown in Table 6. The negative “ a ” value for all inhibitors at different temperatures indicates that the repulsion exists in the adsorbed molecule layer on the metal surface.

Table 6. Adsorption parameters obtained from Temkin adsorption isotherm for corrosion inhibition effect of aqueous leaf extract of SA on mild steel in 1.0 M HCl.

Inhibitor System	Temperature (K)	R ²	Slope	Intercept	− a	K_{ads}	− ΔG^0_{ads} (KJ/mol)
SA	303	0.9469	0.3942	0.5035	2.92	18.93	17.532
	313	0.9859	0.4164	0.3833	2.76	8.32	15.972
	323	0.8519	0.3264	0.4085	2.81	6.295	15.731
	333	0.9378	0.6657	0.3153	2.97	2.97	14.143

The R^2 values at different temperatures are slightly <9 for some inhibitor and approach unity for other inhibitors. It indicates the weak correlation between θ and $\log C$ for the studied inhibitor systems. The value, $R^2 > 0.9$ for same inhibitor and $R^2 < 0.9$ for some other inhibitor systems. The comparison of regression co-efficient, R^2 values indicates that Langmuir isotherm is highly fitting than the Temkin isotherm for the evaluated set of green inhibitors, reflecting that the studied inhibitors follows Langmuir adsorption isotherm more closely than the Temkin isotherm. The high values of K_{ads} and low negative ΔG^0_{ads} values at temperature ranging from 303–303 K (Table 6) indicate that the physisorption occurs. However, chemisorption may not be excluded because of the nature of complex formation in the corrosion-inhibiting process [42].

3.4. Thermodynamic Adsorption Parameter

3.4.1. Free Energy Adsorption (ΔG^0_{ads})

The free energy of adsorptions, ΔG^0_{ads} at different temperature for various concentrations, are determined by Langmuir adsorption isotherm (best fit) model using the Equation:

$$\Delta G^0_{ads} = -2.303 RT \log (K_{ads} \times 55.55) \quad (16)$$

The evaluated mean value of ΔG^0_{ads} at different temperatures is clearly listed (Table 7).

Table 7. Average free energy of adsorption parameters for inhibition effect of corrosion of mild steel at different temperatures in 1.0 M HCl for various concentrations of SA.

Inhibitor System	ΔG^0_{ads} (kJ/mol ^{−1})			
	303	313	323	333
SA-LE	15.027	14.706	14.725	11.102

The negative ΔG^0_{ads} values indicate the occurrence of spontaneous adsorption of inhibitor molecules from the leaves extracts on the mild steel surface. The ΔG^0_{ads} values are up to -20 kJ mol^{-1} and the values are consistent with the physisorption.

3.4.2. Enthalpy and Entropy of Adsorption for Corrosion Process

According to Gibbs Helmholtz relation, a plot of mean value of ΔG^0_{ads} against the temperature is linear with correlation co-efficient value 1 for the corrosion of metal surface in the presence of inhibitor at different concentrations. Plots of ΔG^0_{ads} vs. T is linear with $R^2 > 0.9$ for the corrosion of mild steel in 1.0 M HCl in the presence of the studied inhibitors at different concentrations and at different temperatures. The slope of the straight line and intercept are equal to entropy and enthalpy change in adsorption respectively (Figure 6).

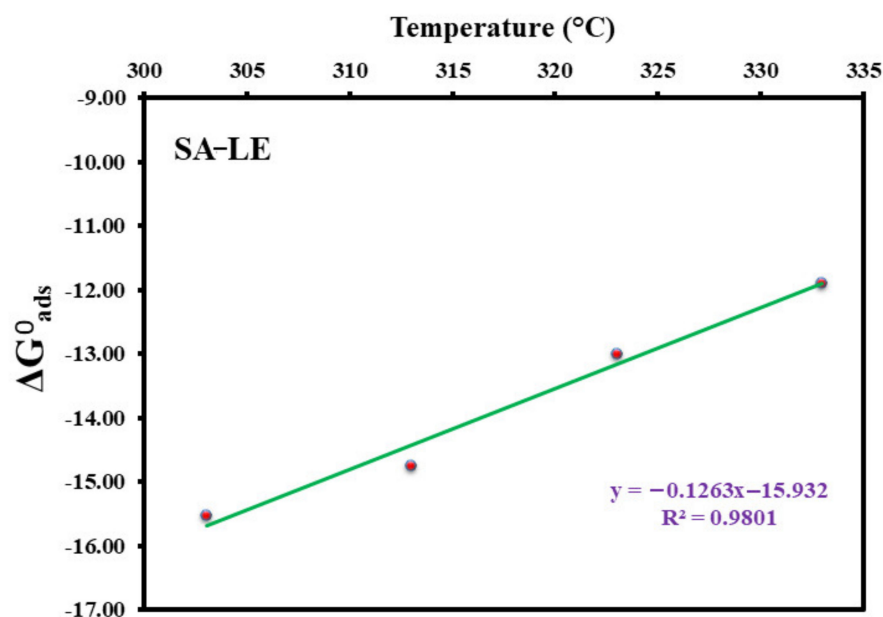


Figure 6. Plot of ΔG_{ads}^0 vs. T for mild steel in aqueous leaf extract of 10% SA at different temperatures.

The mean values ΔH_{ads}^0 and ΔS_{ads}^0 in the temperature range 303–333 K, calculated using the Equation of Gibbs Helmholtz Equation are listed (Table 8).

Table 8. ΔH_{ads}^0 and ΔS_{ads}^0 temperature range in 1.0 M HCl for SA leaf aqueous extract.

Inhibitor System	Mean Values	
	$-\Delta H_{ads}^0$ KJ/mol	$-\Delta S_{ads}^0$ J/mol
SA-LE	15.932	126.3

The negative sign of ΔH_{ads}^0 indicates the exothermic nature (releasing of heat energy) of inhibition of the mild steel dissolution [43]. The ΔH_{ads}^0 value is less than $41.86 \text{ KJ/mol}^{-1}$ showing that the adsorption process is physisorption [41]. The negative sign of ΔS_{ads}^0 for all the studied inhibitors in 1.0 M HCl implies that the molecules from leaves extracts, moving freely in the bulk solution, becomes stationary on the metal surface after the adsorption process, resulting in a decrease of entropy [44]. The large and negative entropy of adsorption suggests that the activated complex formation involves an association mechanism rather than the dissociation mechanism [45].

3.5. Activation Parameter for Corrosion Inhibition Process

Energy of Activation (E_a)

The energy of activation for the corrosion of mild steel in 1.0 M HCl is determined using the Arrhenius type of plot using the Equation $\log CR = K \exp(-E_a/RT)$ and shown in Figure 7.

From the slope of $(-E_a/2303 R)$ of Arrhenius plots, the E_a value is determined and listed in Table 9. In the present investigation, compared to the blank, the E_a values are high at higher concentrations of the inhibitor indicating that it will be more effective at low temperature. Hence the inhibition efficiencies become less and the corrosion rate will be more at high temperatures [46].

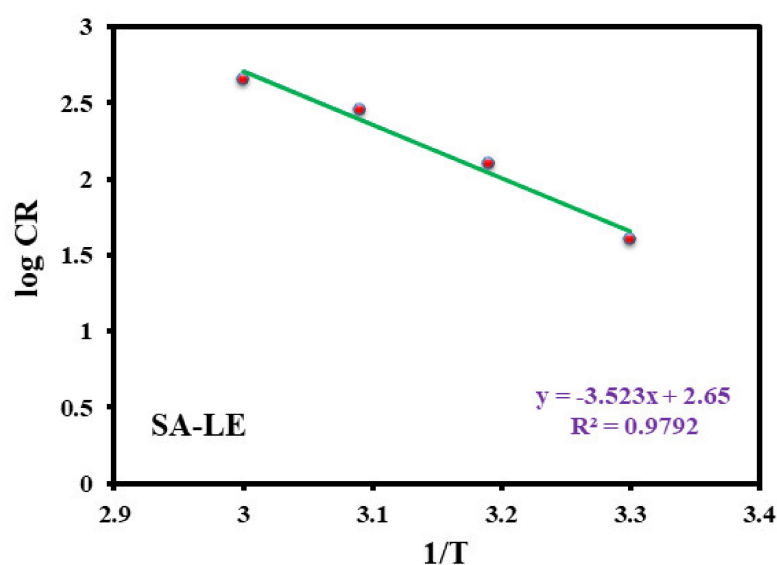


Figure 7. Arrhenius plot for corrosion of mild steel in 1.0 M HCl for solution with 10% SA-LE inhibitor.

Table 9. Average activation energy for corrosion of mild steel in 1.0 M HCl in the absence and in the presence of SA-LE leaf aqueous extract (10% v/v).

Inhibitor System	Ea (KJ/mol)
–	24.30
SA-LE	67.45

Because the inhibitor desorption, greater surface area of mild steel comes in contact to the environment at higher temperature. But this problem is reduced in low temperature because the degree of surface coverage of mild steel becomes close saturation [47].

3.6. Electrochemical Methods

Potentiodynamic Polarization Method

The Tafel plots, obtained from the potentiodynamic polarization study for the inhibition of corrosion of mild steel in 1.0 M HCl by the addition of lower (2% v/v) and high concentrations (10% v/v) of the studied inhibitor SA-LE are shown in Figure 8.

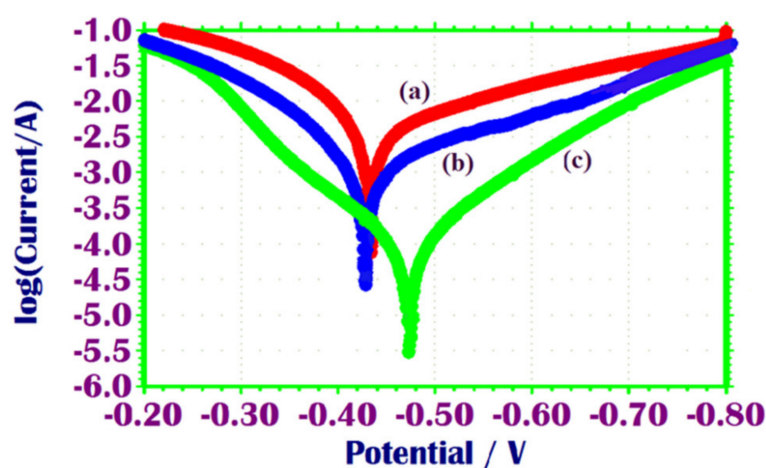


Figure 8. Potentiodynamic polarization curves for corrosion of mild steel in 1.0 M HCl (a) without inhibitor (b) with 2% and (c) with 10% aqueous leaf extract of SA.

Note: scan rate (V/s) = 0.01, initial E(V) = −0.8, final E(V) = −0.2, hold time at E f (S) = 0 and quiet Time (S) = 2.

The potentiodynamic polarization parameters such as corrosion current density (I_{corr}), corrosion potential (E_{corr}), anodic (b_a), cathodic (b_c) Tafel slopes, LPR (R_p) obtained from the extrapolation of the polarization plots for the corrosion of mild steel in the presence of low and high concentrations of extracts of SA-LE and also for the blank solution, are given in Table 10.

Table 10. Potentiodynamic polarization parameters for the corrosion of mild steel in 1.0 M HCl without and with various concentrations of SA leaf aqueous extract.

Concentration of the Leaves Extract (% v/v)	$-E_{\text{corr}}$ mV/SCE	Tafel Slope		I_{corr} mA/cm ²	R_p $\Omega\cdot\text{cm}^2$	Inhibition Efficiency (%) Calculated From:	
		b_a mV/dec	b_c mV/dec			I_{corr} mA/cm ²	R_p $\Omega\cdot\text{cm}^2$
0	−434	140	232	6.488×10^{-3}	5.9	—	—
2	−429	10	225	1.527×10^{-3}	20.4	76.4	71.0
10	−473	108	096	1.024×10^{-4}	216	98.4	97.2

When leaf extract is added to a corrosive solution I_{corr} values decrease for all the studied inhibitors than the solutions without inhibitor. This proves the inhibitive action of the extracts on mild steel corrosion in 1.0 M HCl. The reduction of corrosion current density in the presence of the inhibitor shows that the inhibitors are adsorbed on the surface of the metal and inhibit corrosion. The increase in cathodic and anodic Tafel slopes (b_c & b_a) with increasing inhibitor concentrations show that both the anodic and cathodic reactions are controlled by the inhibitor solutions [48]. The linear polarization resistance value (R_p) increases from 5.9 $\Omega\cdot\text{cm}^2$ (blank) to high values with increasing the concentration of inhibitor and it indicates the formation of a protective film on the surface of the metal. In addition to this, further analyses of the samples have also been performed using electrochemical impedance spectroscopy, the Nyquist plots and Bode plots are provided in the supplementary information (Figures S1–S4 and Table S3). The results of electrochemical impedance indicated the adsorption of the phytochemical components of leaf extract on the surface of mild steel and the formation of film at the interface of metal/solution. The Bode plots revealed that the adsorption of the inhibitor on mild steel surface occurs in a single process.

3.7. Surface Analytical Methods

3.7.1. Atomic Force Microscopy (AFM)

The 3D AFM morphologies and the AFM cross sectional profiles of polished mild steel and mild steel after immersion in 1.0 M HCl for 2 h at room temperature, are shown in Figure 9a,b.

The AFM cross sectional images of the mild steel coupon after being immersed for 2 h at room temperature in 1.0 M HCl in the presence of the high concentrations of SA-LE is shown in Figure 10.

The different parameters R_q , R_a , and R_y from the AFM images of metal surfaces are given in Table 11 for the polished mild steel and that after immersion in the absence and presence of 10% of the inhibitor SA-LE. The analysis of values indicates that the average roughness R_a values, after the mild steel is immersed in 1.0 M HCl in the presence of inhibitor at high concentration, lies in between the blank and polished mild steel. It can be inferred that a protective film is formed on the surface of the metal. For the blank system (Figure 10), a few pits in the corroded metal surface are observed and the slight roughness is noted on the polished steel surface (Figure 9). The surface topography of the metal surfaces, in the presence of high concentrations of inhibitor, show that the (P-V) height is greater for the inhibited system compared to the polished system and less than that of

the blank system. These observations prove that the surface is smoother, in presence of inhibitor because of the layer formation and also the protective film is in nanometer scale of all the inhibitors SA-LE in 1.0 M HCl.

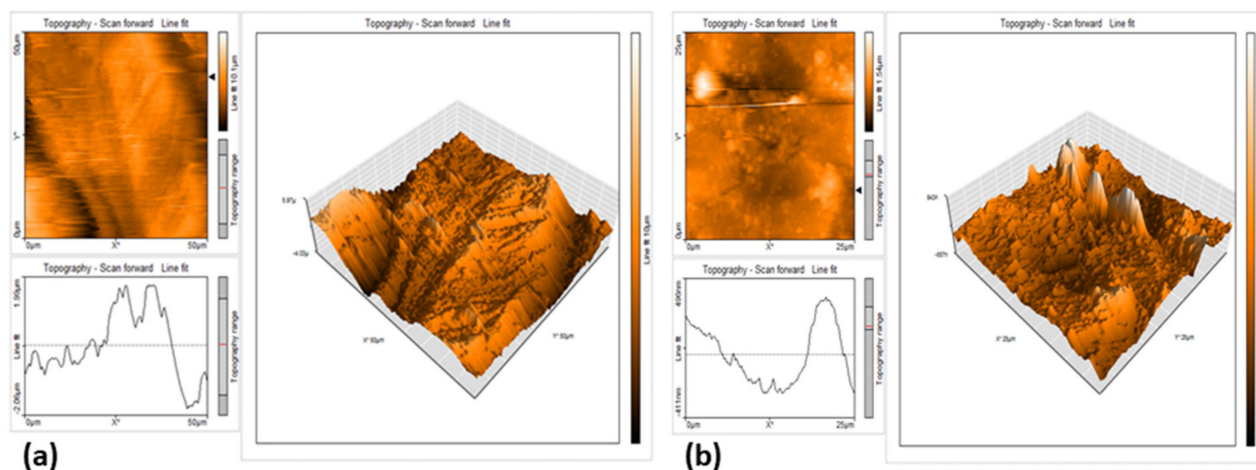


Figure 9. (a). AFM cross sectional images of the polished mild steel surface and (b) AFM cross sectional images of the mild steel surface after immersion in 1.0 M HCl.

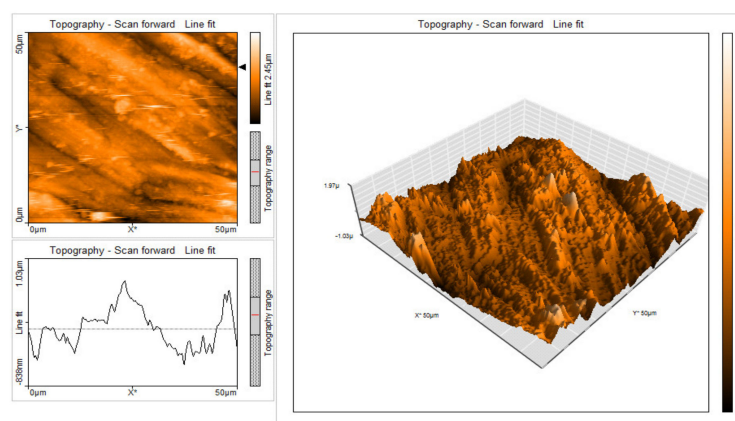


Figure 10. AFM cross sectional image for the mild steel surface after immersion in 1.0 M HCl with the 10% aqueous SA leaf extract.

Table 11. AFM surface and line roughness data for different systems.

System	Surface Roughness			Line Roughness		
	Average Roughness (R_a), nm	Root Mean Square Roughness (R_q), nm	Maximum Peak to Valley (P-V) Height, nm	Average Roughness (R_a), nm	Root Mean Square Roughness (R_q), nm	Maximum Peak to Valley (P-V) height, nm
Polished mild steel	117.5	162.7	171.5	64.1	76.9	359.0
Mild steel + 1.0 M HCl+ 10% of aqueous leaf extract SA	229.7	289.3	2524.1	185.9	221.3	1201.2
Mild steel + 1.0 M HCl	847.8	1086.9	8393.5	828.2	1084	4511.9

3.7.2. Scanning Electron Microscope Analysis (SEM)

In the present evaluation, the SEM micrograph of the polished mild steel specimen index in the protected condition has been recorded at 8.29 kX magnification and it is presented in Figure 11a,b. The SEM micrograph of the mild steel specimen, after immersion in the 1.0 M HCl for 2 h at room temperature, is taken and the image is shown in Figure 11c.

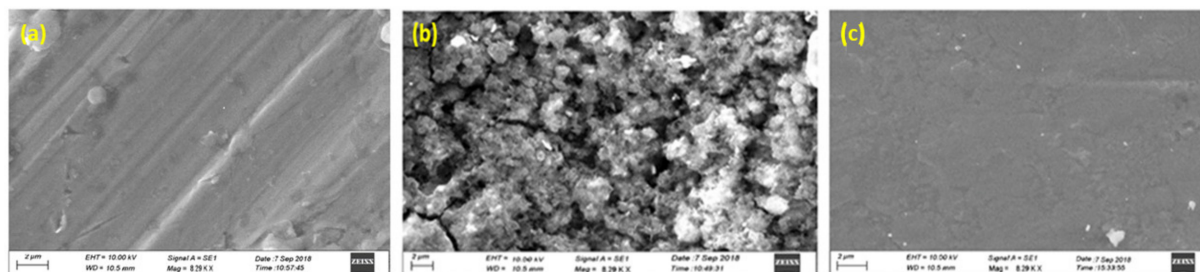


Figure 11. (a) SEM image of polished mild steel coupon before immersion in 1.0 M HCl, (b) SEM image of mild steel coupon after immersion in 1.0 M HCl (2 h), and (c) SEM image of polished mild steel coupon after immersion in 1.0 M HCl in the presence of 10% aqueous leaf extract of SA.

It reveals the complete destruction or deterioration of the smoothness of the metal surface and formation of corrosion spots. The image shows that due to the corrosion, the metal surface is highly damaged. The SEM micrograph of the mild steel specimen after immersion period for 2 h at room temperature in 1.0 M HCl solution in presence of SA-LE inhibitor at higher concentration (10%) is shown in (Figure 11c).

The SEM micrograph image of the mild steel samples immersed in 1.0 M HCl with inhibitor shows lesser degree of surface deterioration than those for mild steel coupon immersed in 1.0 M HCl without inhibitor. The SEM micrograph image (Figure 11) of the external topography of the surface of the mild steel samples, immersed in 1.0 M HCl with inhibitor show that the corroded scales (areas) are spread on the mild steel irregularly to some extent and display a definite level of firmness which cannot be removed off easily [49]. Thus it is revealed that the inhibitor has increased the efficiency of adsorption at the metal/solution interface and thus the inhibitors tend to reduce metallic surface destruction.

3.7.3. Contact Angle Measurements

The contact angle is the angle, conventionally measured through the liquid, where a liquid–vapor interface meets on the solid surface. It quantifies the wettability of a solid surface by a liquid. In order to verify the adsorption nature of the inhibitor on the surface of the corrosive metal, the contact angle is determined. The observed contact angle is very high for the polished mild steel (Figure 12a) which indicates the hydrophilicity behavior at the angle of 145° . The contact angle of 145° characterizes a surface with water repellant nature. For the comparison, the contact angle also measured for the surface of mild steel after immersion in the corrosive solution of 1.0 M HCl without the presence of inhibitor for the immersion period of 2 h at room temperature is determined to be 38.1° (Figure 12b). It shows that the wettability nature of metal surface increases in the presence of 10% SA-LE inhibitor, Figure 12c. Increase in contact angle 129.7° revealing the formation of a hydrophobic layer due to the adsorption of plant components onto the metal surface [50].

In the presence of the inhibitors, larger contact angles are observed. Because of this development the surface becomes water repellant with less wettability. So, the inhibition efficiency increases in the presence of the inhibitors [51]. The observed value of contact angle for system is given in Table 12.

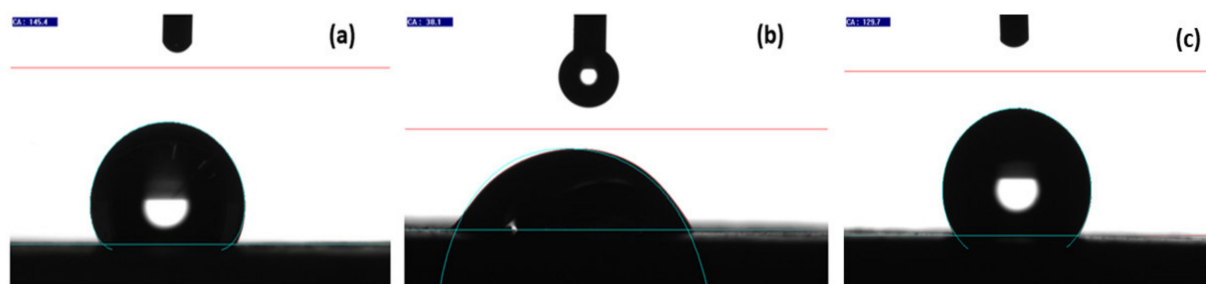


Figure 12. (a) Contact angle measurement on the polished mild steel surface, (b) contact angle measurement for the mild steel surface that is kept for 2 h in a 1.0 M HCl solution without inhibitor and (c) contact angle measurements on the mild steel surface that is kept for 2 h in a 1.0 M HCl solution containing 10% aqueous leaf extract of SA.

Table 12. Contact angle values measured for different systems.

System	Contact Angle (°)
Mild steel + 1.0 M HCl	38.1
Mild steel + 1.0 M HCl + 10% of SA-LE	129.7
Polished mild steel	145.4

3.7.4. FT-IR Spectral Studies

FT-IR Results for SA-LE/Mild Steel/1.0 M HCl

The FT-IR spectral patterns of the crude SA-LE and scratched film from the surface of the mild steel after immersion in 1.0 M HCl with highest concentration (10% *v/v*) of extract of SA-LE are given (Figures S5 and S6, Supplementary File). The respective absorption bands are given in Table S2, Supplementary File.

The shifts in IR peak 3401 cm^{-1} to 3431 cm^{-1} shows the presence of O–H groups. The peak 2924 cm^{-1} shifts to 2855 cm^{-1} and 2854 cm^{-1} to 2924 cm^{-1} indicating the C–H stretching. The peaks at 1742 , 1560 , and 1113 cm^{-1} are not noticed in adsorbed layer. It shows that the C=O, C=C, C–O groups may be involved in the formation of barrier layer [52]. The new peaks at 471 and 571 cm^{-1} are observed for the scratched film from the surface of mild steel immersed in 1.0 M HCl with 10% SA-LE extract and it shows the Fe-complex present in the adsorbed layer on the surface of mild steel.

UV-Visible Spectral Analysis

The extracts prepared from plant leaves, have many constituents and are responsible for the inhibition of metal corrosion. The chemical constituents, present in the extract, are expected to form complex with the surface of metal during the process of inhibition. The complexes produced are revealed by the analysis of UV-visible spectrum. During corrosion in 1.0 M HCl acid solution, metal cations are expected to be formed on the surface of the metal, which leads to the formation of complexes with phytochemical constituents of SA-LE [45].

The changes in the positions of absorption maxima and the absorbance values reveal the complex formation between the ions on the metal surface and SA-LE inhibitor [53]. The pattern of the UV-visible absorption spectra is recorded for the crude SA-LE and the solution of the mixture of mild steel 1.0 M HCl/10% concentration of the SA-LE inhibitor after 2 h duration (Figure 13).

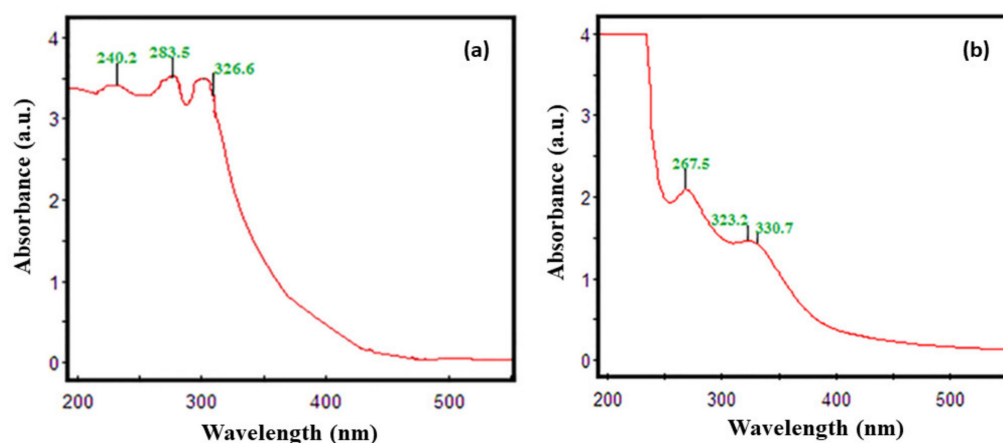


Figure 13. (a) UV-visible spectra of aqueous SA-LE and (b) the scratched film from mild steel after immersion in 1.0 M HCl with 10% SA-LE inhibitor.

A change in the values of absorbance and the corresponding intensities were observed (Figure 13). The shifting of absorption bands may be due to the $\pi-\pi^*$ and $n-\pi^*$ transitions along with a significant charge transfer character. The deviation in the maximum absorption and the intensity values represent the complex formation between Fe^{2+} and phyto-components of the SA-LE [54].

The UV-visible spectral pattern exhibits the possibility of interaction between the hetero atoms present in the leaf extract and metal ion from the metal surface [55]. The data of UV-visible spectra show that the bands in the region 200 to 350 nm are due to the carbonyl groups held close to Fe in the complex forms [53]. It reveals complex formation between the cation from the surface of the metal and phyto-components from SA-LE, which is responsible for the anticorrosive properties of leaves extract. This assumption is also supported by the FT-IR analysis and has also been reported in earlier studies [56].

3.8. Phyto-Constituents of SA-LE

The phytochemical screening of the leaf extract of SA shows the presence of active components such as alkaloids, tannins, flavonoids, glycosides, phenolic compounds, and carbohydrates [57]. The main pungent constituent reported in it is spilanthol, which is an isobutyl amide [58]. The secondary metabolites present in the SA-LE are spilanthol, Undeca-2F-7Z,9E-trienoic isobutyl amide, undeca-2E-en-8,10-diyonic acid isobutyl-amide, 2E-N-(2-methylbutyl-2-undecane-8,10-diynamide, 2E-7Z-N-isobutyl-2,7-tridecadiene-10, 12-diynamide, 7Z-N-isobutyl-7-tridecene-10, 12-diynamide, β -sitosterol, stigmasterol, α -Amyrin, β -Amyrin, limonene, 3-acetylaleuritolic acid, vanillic acid, β -sitostenone, scopoletin, trans-ferulic acid, trans-isoferulic acid etc. These components contain O, N, and aromatic ring in their molecular structures. The organic heterogeneous compounds containing adsorption active centers such as O, N, and aromatic ring, have been reported to be efficient corrosion inhibitor [59]. The adsorption takes place through these active centers involving complex formation with the cation of metal. The surface of the metal may be blocked by these complexes and thus the rate of corrosion is reduced.

3.9. Corrosion Inhibition Mechanism

The adsorption of leaves extract is caused by the adsorption of phytochemical components contained in the leaf extract on the metal surface, which prevents the surface of the metal from the attack by acid and thus does not allow the corrosion action to occur [60]. The retardation of anodic dissolution in the presence of an inhibitor molecule has been described by the mechanism involving two adsorbed intermediate. It is a known fact that mild steel has coordination affinity to sulfur, nitrogen, and oxygen-containing ligands (cf. Figure 14) [61]. The atoms such as N, O, and S are capable of forming coordinate covalent bonds with metal owing to their free electron pairs and thus act as inhibitors [62]. The process may block

the active sites and hence decrease the corrosion rate. The aqueous leaf extract contains these atoms in their phyto-constituents and could be adsorbed on the surface of the metal and reduce the surface area available for a cathodic and anodic corrosion reaction to take place. In acidic solution, the active constituents present in the inhibitor exist as protonated species and adsorb on the cathodic sites of mild steel reducing the evolution of hydrogen. The adsorption on anodic sites occurs through π electrons and lone pair of electrons on hetero atom of the active components present in the inhibitor. For example, leaves extract of *S. officinalis* exhibited decent corrosion inhibition activity on 304 stainless steel in 1 M HCl solution because of the adsorption of phenolic components such as luteolin 7-glucuronide, carnosol, sagecomarin, etc., [63], through their heteroatoms including N and O, which acted as effective adsorption centers. *Osmanthus fragran* leaves extract has shown mixed type corrosion inhibition activity against carbon steel in 1 M HCl [64]. In another study, alkaloids extract of *Geissospermum* leaf has also demonstrated mixed type inhibition activity on C38 steel in 1 M HCl, which is revealed by Langmuir adsorption isotherm [65]. Indeed, the leave extract has achieved a maximum inhibition efficiency of ~92% at 100 mg/L concentration. Notably, the phytochemical constituents typically contain different variety of phytomolecules, therefore, in most of the cases Langmuir mixed type of corrosion inhibition activity is observed [9].

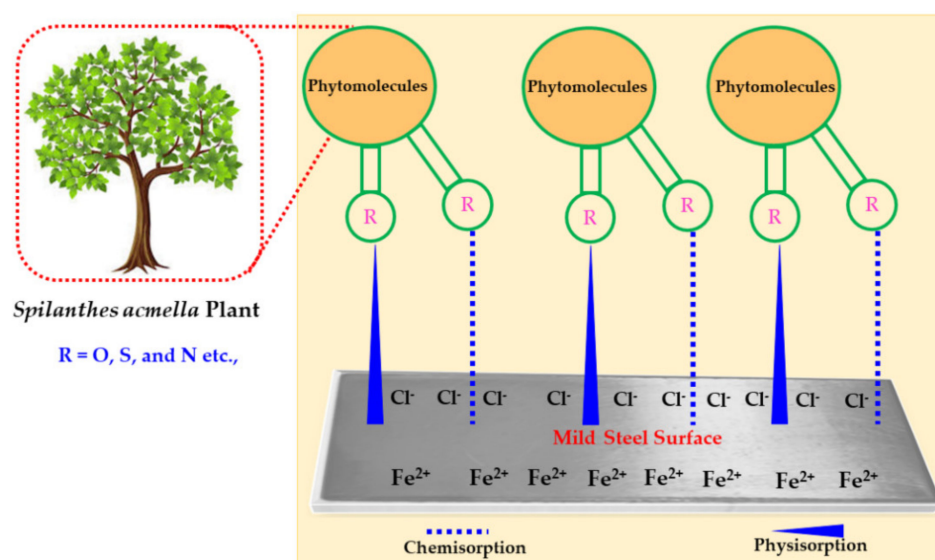


Figure 14. Schematic representation of tentative corrosion inhibition mechanism.

4. Conclusions

In this study, the anticorrosion properties of the SA-LE have been tested against the mild steel in acidic solution. The preliminary phytochemical screening of SA-LE has indicated the presence of various chemical constituents including alkaloids, flavonoids, and other phenolic compounds with hetero atomic centers. Weight loss measurements of mild steel coupons in the presence and absence of SA-LE in 1.0 M HCl medium suggest that the percentage of inhibition efficiency increases progressively with increasing inhibitor concentrations. Besides with increasing temperatures from 303 K–333 K the inhibition efficiency decreased because of the partial desorption of the barrier layer from the metal surface. The calculated high K_{ads} and low negative ΔG^0_{ads} values from the Langmuir isotherm indicate that the adsorption of inhibitor molecules from the aqueous leaf extract on the mild steel surface happens spontaneously which is consistent with physisorption. However, the chance of complex formation during the corrosion inhibition does not exclude chemisorption. The Nyquist plots of electrochemical impedance suggest the adsorption of the phytochemical components of leaf extract on the surface of mild steel and the formation of film at the interface of metal/solution. The Bode plots revealed that the adsorption of the

inhibitor on mild steel surface occurs in a single process. Furthermore, microscopic studies including SEM and AFM have indicated the presence of smooth surface in case of inhibited mild steel when compared to the uninhibited samples. Additionally, the evaluation of phytochemical constituents suggests that the formation of complex between surface ions (Fe^{+}) and inhibitor on the surface of the metal possibly help prevent the corrosion process. The investigated SA leaves extract acted as efficient corrosive inhibitor of mild steel in acidic medium.

Supplementary Materials: The following are available online at <https://www.mdpi.com/2079-6412/11/1/106/s1>, Figure S1. Nyquist plot for the corrosion of (a) mild steel in 1.0 M HCl without inhibitor (b) with 2% and (c) with 10% aqueous leaf extract of SA. Figure S2. Bode plots for the corrosion of mild steel in 1.0 M HCl without inhibitor. Figure S3. Bode plots for the corrosion of mild steel in 1.0 M HCl with 2% SA-LE inhibitor. Figure S4. Bode plots for the corrosion of mild steel in 1.0 M HCl with 10% SA-LE inhibitor. Figure S5. FT-IR spectrum of aqueous leaf extract of SA. Figure S6. FT-IR spectrum of scratched film from the mild steel surface after immersion in 1.0 M HCl in the presence of 10% aqueous leaf extract of SA. Table S1. FT-IR spectral data of aqueous extract of SA leaves. Table S2. FT-IR Spectral data for the aqueous leaf extract of SA and the scratched film from mild steel surface after immersion in 1.0 M HCl with 10% SA. Table S3. Electrochemical impedance parameters from Nyquist plot and bode plot for the corrosion of mild steel without and with the various concentrations of aqueous SA leaves extract in 1.0 M HCl.

Author Contributions: Conceptualization, A.A.S.B. and V.K.; data curation, A.A.S.B., R.M.A.V., V.K., and M.R.S.; formal analysis, A.A.S.B., R.M.A.V., V.K., M.R.S., A.A., and E.M.A.; investigation, A.A.S.B., R.M.A.V., V.K., and E.M.A.; methodology, A.A.S.B., and V.K.; visualization, M.R.S.; writing—original draft, A.A.S.B., R.M.A.V., V.K., M.K., and M.R.S.; writing—review and editing, A.A.S.B., R.M.A.V., V.K., M.K., and M.R.S. All authors have read and agreed to the published version of the manuscript.

Funding: The authors extend their appreciation to the Deanship of Scientific Research at King Saud University for funding this work through Research Group no. RG-1441-453.

Institutional Review Board Statement: Not applicable.

Informed Consent Statement: Not applicable.

Data Availability Statement: Data is contained within the article or Supplementary material.

Acknowledgments: The authors extend their appreciation to the Deanship of Scientific Research at King Saud University for funding this work through Research Group no. RG-1441-453.

Conflicts of Interest: The authors declare that they have no conflict of interest.

References

1. Ukoba, O.; Oke, P.; Ibegbulam, M. Corrosion Behaviour of Ductile Iron in Different Environment. *Int. J. Sci. Technol.* **2012**, *2*, 618–621.
2. Chen, Y.; Hong, T.; Gopal, M.; Jepson, W. EIS studies of a corrosion inhibitor behavior under multiphase flow conditions. *Corros. Sci.* **2000**, *42*, 979–990. [[CrossRef](#)]
3. Riggs, O.L., Jr.; Hurd, R.M. Temperature coefficient of corrosion inhibition. *Corrosion* **1967**, *23*, 252–260. [[CrossRef](#)]
4. Chigondo, M.; Chigondo, F. Recent natural corrosion inhibitors for mild steel: An overview. *J. Chem.* **2016**, *2016*, 1–7. [[CrossRef](#)]
5. Oyekunle, D.; Agboola, O.; Ayeni, A. *Corrosion Inhibitors as Building Evidence for Mild Steel: A Review*; Journal of Physics: Conference Series; IOP Publishing: Bristol, UK, 2019; p. 032046.
6. Dwivedi, D.; Lepková, K.; Becker, T. Carbon steel corrosion: A review of key surface properties and characterization methods. *RSC Adv.* **2017**, *7*, 4580–4610. [[CrossRef](#)]
7. Zaferani, S.H.; Sharifi, M.; Zaarei, D.; Shishesaz, M.R. Application of eco-friendly products as corrosion inhibitors for metals in acid pickling processes-A review. *J. Environ. Chem. Eng.* **2013**, *1*, 652–657. [[CrossRef](#)]
8. Raja, P.B.; Sethuraman, M.G. Natural products as corrosion inhibitor for metals in corrosive media-A review. *Mater. Lett.* **2008**, *62*, 113–116. [[CrossRef](#)]
9. Verma, C.; Ebenso, E.E.; Bahadur, I.; Quraishi, M. An overview on plant extracts as environmental sustainable and green corrosion inhibitors for metals and alloys in aggressive corrosive media. *J. Mol. Liq.* **2018**, *266*, 577–590. [[CrossRef](#)]
10. Sanyal, B. Organic compounds as corrosion inhibitors in different environments-A review. *Prog. Org. Coat.* **1981**, *9*, 165–236. [[CrossRef](#)]

11. Mo, S.; Luo, H.-Q.; Li, N.-B. Plant extracts as “green” corrosion inhibitors for steel in sulphuric acid. *Chem. Pap.* **2016**, *70*, 1131–1143. [\[CrossRef\]](#)
12. Fang, Y.; Suganthan, B.; Ramasamy, R.P. Electrochemical characterization of aromatic corrosion inhibitors from plant extracts. *J. Electroanal. Chem.* **2019**, *840*, 74–83. [\[CrossRef\]](#)
13. Miralrio, A.; Espinoza Vázquez, A. Plant Extracts as Green Corrosion Inhibitors for Different Metal Surfaces and Corrosive Media: A Review. *Processes* **2020**, *8*, 942. [\[CrossRef\]](#)
14. Umoren, S.A.; Solomon, M.M.; Obot, I.B.; Suleiman, R.K. A critical review on the recent studies on plant biomaterials as corrosion inhibitors for industrial metals. *J. Ind. Eng. Chem.* **2019**, *76*, 91–115. [\[CrossRef\]](#)
15. El Ibrahim, B.; Jmair, A.; Bazzi, L.; El Issami, S. Amino acids and their derivatives as corrosion inhibitors for metals and alloys. *Arab. J. Chem.* **2020**, *13*, 740–771. [\[CrossRef\]](#)
16. Raja, P.B.; Fadaeinasab, M.; Qureshi, A.K.; Rahim, A.A.; Osman, H.; Litaudon, M.; Awang, K. Evaluation of green corrosion inhibition by alkaloid extracts of *Ochrosia oppositifolia* and *isoreserpiline* against mild steel in 1 M HCl medium. *Ind. Eng. Chem. Res.* **2013**, *52*, 10582–10593. [\[CrossRef\]](#)
17. Morad, M.S.S.; Hermas, A.E.H.A.; Aal, M.S.A. Effect of amino acids containing sulfur on the corrosion of mild steel in phosphoric acid solutions polluted with Cl[−], F[−] and Fe³⁺ ions—behaviour near and at the corrosion potential. *J. Chem. Technol. Biotechnol. Int. Res. Process Environ. Clean Technol.* **2002**, *77*, 486–494. [\[CrossRef\]](#)
18. Olivares-Xometl, O.; Likhanova, N.; Domínguez-Aguilar, M.; Arce, E.; Dorantes, H.; Arellanes-Lozada, P. Synthesis and corrosion inhibition of α -amino acids alkylamides for mild steel in acidic environment. *Mater. Chem. Phys.* **2008**, *110*, 344–351. [\[CrossRef\]](#)
19. Dubey, S.; Maity, S.; Singh, M.; Saraf, S.A.; Saha, S. Phytochemistry, pharmacology and toxicology of *Spilanthes acmella*: A review. *Adv. Pharmacol. Sci.* **2013**, *2013*, 1–9.
20. Dias, A.; Santos, P.; Seabra, I.; Júnior, R.; Braga, M.; De Sousa, H. Spilanthol from *Spilanthes acmella* flowers, leaves and stems obtained by selective supercritical carbon dioxide extraction. *J. Supercrit. Fluids* **2012**, *61*, 62–70. [\[CrossRef\]](#)
21. Elufioye, T.O.; Habtemariam, S.; Adejare, A. Chemistry and Pharmacology of Alkylamides from Natural Origin. *Rev. Bras. Farmacogn.* **2020**, *30*, 1–19. [\[CrossRef\]](#)
22. Durodola, S.S.; Adekunle, A.S.; Olasunkanmi, L.O.; Oyekunle, J.A. Inhibition of Mild Steel Corrosion in Acidic Medium by Extract of *Spilanthes Uliginosa* Leaves. *Electroanalysis* **2020**, *32*, 2693–2702. [\[CrossRef\]](#)
23. Macdonald, J.R. Impedance spectroscopy: Emphasizing solid materials and systems. *Appl. Opt.* **1989**, *28*, 1083.
24. Towfri, L.; Kadri, A.; Khelifa, A.; Aimeur, N.; Benlrahim, N. The inhibition and adsorption processes of L-cysteine against the corrosion of XC 18 carbon Steel in 2N H₂SO₄. *J. Eng. Appl. Sci.* **2008**, *3*, 688–696.
25. Satapathy, A.; Gunasekaran, G.; Sahoo, S.; Amit, K.; Rodrigues, P. Corrosion inhibition by *Justicia gendarussa* plant extract in hydrochloric acid solution. *Corros. Sci.* **2009**, *51*, 2848–2856. [\[CrossRef\]](#)
26. Vankar, P.S.; Srivastava, J. Comparative study of total phenol, flavonoid contents and antioxidant activity in *Canna indica* and *Hibiscus rosa sinensis*: Prospective natural food dyes. *Int. J. Food Eng.* **2008**, *4*. [\[CrossRef\]](#)
27. Acharya, J.; Sahu, J.; Sahoo, B.; Mohanty, C.; Meikap, B. Removal of chromium (VI) from wastewater by activated carbon developed from Tamarind wood activated with zinc chloride. *Chem. Eng. J.* **2009**, *150*, 25–39. [\[CrossRef\]](#)
28. Li, X.; Deng, S.; Fu, H. Inhibition of the corrosion of steel in HCl, H₂SO₄ solutions by bamboo leaf extract. *Corros. Sci.* **2012**, *62*, 163–175. [\[CrossRef\]](#)
29. Yadav, R. Phytochemical Screening of *Spilanthes acmella* plant parts. *Int. J. Pharm. Erud.* **2012**, *1*, 44–72.
30. Harborne, A. *Phytochemical Methods a Guide to Modern Techniques of Plant Analysis*; Springer Science & Business Media: Berlin, Germany, 1998.
31. Nabi, N.G.; Wani, T.A.; Shrivastava, M.; Rashid, A.; Shah, S. *Spilanthes acmella* an endangered medicinal plant-its Traditional, Phytochemical and Therapeutic properties-An overview. *Int. J. Adv. Res.* **2016**, *4*, 627–639.
32. Cheng, Y.-B.; Liu, R.H.; Ho, M.-C.; Wu, T.-Y.; Chen, C.-Y.; Lo, I.-W.; Hou, M.-F.; Yuan, S.-S.; Wu, Y.-C.; Chang, F.-R. Alkylamides of *Acemella oleracea*. *Molecules* **2015**, *20*, 6970–6977. [\[CrossRef\]](#)
33. Akalezi, C.O.; Enenebaku, C.K.; Oguzie, E.E. Inhibition of acid corrosion of mild steel by biomass extract from the *Petersianthus macrocarpus* plant. *J. Mater. Environ. Sci.* **2013**, *4*, 217–226.
34. Solmaz, R.; Mert, M.; Kardaş, G.; Yazici, B.; Erbil, M. Adsorption and corrosion inhibition effect of 1, 1'-thiocarbonyldiimidazole on mild steel in H₂SO₄ solution and synergistic effect of iodide ion. *Acta Phys. Chim. Sin.* **2008**, *24*, 1185–1191. [\[CrossRef\]](#)
35. Singh, A.K.; Quraishi, M. Effect of 2, 2' benzothiazolyl disulfide on the corrosion of mild steel in acid media. *Corros. Sci.* **2009**, *51*, 2752–2760. [\[CrossRef\]](#)
36. Noor, E.A.; Al-Moubaraki, A.H. Thermodynamic study of metal corrosion and inhibitor adsorption processes in mild steel/1-methyl-4 [4'(-X)-styryl pyridinium iodides/hydrochloric acid systems. *Mater. Chem. Phys.* **2008**, *110*, 145–154. [\[CrossRef\]](#)
37. Shao, H.; Wang, J.; Zhang, Z.; Zhang, J.; Cao, C. The cooperative effect of calcium ions and tartrate ions on the corrosion inhibition of pure aluminum in an alkaline solution. *Mater. Chem. Phys.* **2003**, *77*, 305–309. [\[CrossRef\]](#)
38. Sethi, T.; Chaturvedi, A.; Upadhyay, R.; Mathur, S. Corrosion inhibitory effects of some Schiff's bases on mild steel in acid media. *J. Chil. Chem. Soc.* **2007**, *52*, 1206–1213. [\[CrossRef\]](#)
39. Refaey, S.; Taha, F.; Abd El-Malak, A. Inhibition of stainless steel pitting corrosion in acidic medium by 2-mercaptobenzoxazole. *Appl. Surf. Sci.* **2004**, *236*, 175–185. [\[CrossRef\]](#)

40. Ebenso, E.E.; Obot, I.B.; Murulana, L. Quinoline and its derivatives as effective corrosion inhibitors for mild steel in acidic medium. *Int. J. Electrochem. Sci.* **2010**, *5*, 1574–1586.
41. Moretti, G.; Guidi, F.; Grion, G. Tryptamine as a green iron corrosion inhibitor in 0.5 M deaerated sulphuric acid. *Corros. Sci.* **2004**, *46*, 387–403. [\[CrossRef\]](#)
42. Ahamad, I.; Prasad, R.; Quraishi, M. Adsorption and inhibitive properties of some new Mannich bases of Isatin derivatives on corrosion of mild steel in acidic media. *Corros. Sci.* **2010**, *52*, 1472–1481. [\[CrossRef\]](#)
43. Shukla, S.K.; Ebenso, E.E. Corrosion inhibition, adsorption behavior and thermodynamic properties of streptomycin on mild steel in hydrochloric acid medium. *Int. J. Electrochem. Sci.* **2011**, *6*, 3277–3291.
44. Gomma, G.K.; Wahdan, M.H. Effect of temperature on the acidic dissolution of copper in the presence of amino acids. *Mater. Chem. Phys.* **1994**, *39*, 142–148. [\[CrossRef\]](#)
45. Obi-Egbedi, N.; Obot, I. Xanthione: A new and effective corrosion inhibitor for mild steel in sulphuric acid solution. *Arab. J. Chem.* **2013**, *6*, 211–223. [\[CrossRef\]](#)
46. Umoren, S.; Ebenso, E.; Okafor, P.; Ogbobe, O. Water-soluble polymers as corrosion inhibitors. *Pigment Resin Technol.* **2006**, *35*, 346–352. [\[CrossRef\]](#)
47. Herrag, L.; Hammouti, B.; Elkadiri, S.; Aouniti, A.; Jama, C.; Vezin, H.; Bentiss, F. Adsorption properties and inhibition of mild steel corrosion in hydrochloric solution by some newly synthesized diamine derivatives: Experimental and theoretical investigations. *Corros. Sci.* **2010**, *52*, 3042–3051. [\[CrossRef\]](#)
48. Benali, O.; Benmehdi, H.; Hasnaoui, O.; Selles, C.; Salghi, R. Green corrosion inhibitor: Inhibitive action of tannin extract of *Chamaerops humilis* plant for the corrosion of mild steel in 0.5 M H₂SO₄. *J. Mater. Environ. Sci.* **2013**, *4*, 127–138.
49. Badawy, W.; Al-Kharafi, F.; El-Azab, A. Electrochemical behaviour and corrosion inhibition of Al, Al-6061 and Al-Cu in neutral aqueous solutions. *Corros. Sci.* **1999**, *41*, 709–727. [\[CrossRef\]](#)
50. Ghareba, S.; Omanovic, S. Corrosion inhibition of carbon steel in sulfuric acid by sodium caprylate. *Balance* **2016**, *100*, 74–84.
51. Hassan, H.; Ismail, A.; Ahmad, S.; Soon, C. *Super-Hydrophobic Green Corrosion Inhibitor on Carbon Steel*; IOP Conference Series: Materials Science and Engineering; IOP Publishing: Bristol, UK, 2017; pp. 1–5.
52. Eddy, N.; Ebenso, E. Corrosion inhibition and adsorption properties of ethanol extract of *Gongronema latifolium* on mild steel in H₂SO₄. *Pigment Resin Technol.* **2010**, *39*, 77–83. [\[CrossRef\]](#)
53. Abboud, Y.; Abourriche, A.; Saffaj, T.; Berrada, M.; Charrouf, M.; Bennamara, A.; Al Himidi, N.; Hannache, H. 2, 3-Quinoxalinedione as a novel corrosion inhibitor for mild steel in 1 M HCl. *Mater. Chem. Phys.* **2007**, *105*, 1–5. [\[CrossRef\]](#)
54. Singh, A.; Ebenso, E.E.; Quraishi, M. Theoretical and electrochemical studies of *Cuminum cyminum* (Jeera) extract as green corrosion inhibitor for mild steel in hydrochloric acid solution. *Int. J. Electrochem. Sci.* **2012**, *7*, 8543–8559.
55. Petchiammal, A.; Selvaraj, S. Investigation of Anti-Corrosive Effects of Lebbeck Seed Extract On Aluminum in Acid Environment. *Pac. J. Sci. Technol.* **2013**, *14*, 31–39.
56. Bothi Raja, P.; Sethuraman, M. Strychnos nux-vomica an eco-friendly corrosion inhibitor for mild steel in 1 M sulfuric acid medium. *Mater. Corros.* **2009**, *60*, 22–28. [\[CrossRef\]](#)
57. Arora, S.; Vijay, S.; Kumar, D. Phytochemical and antimicrobial studies on the leaves of *Spilanthes acmella*. *J. Chem. Pharm. Res.* **2011**, *3*, 145–150.
58. Arif, M.; Juyal, D.; Joshi, A. A review on pharmacognostic and phytochemical study of a plant *Spilanthes acmella* Murr. *Pharma. Innov.* **2017**, *6*, 172.
59. Obot, I.; Ebenso, E.; Gasem, Z.M. Eco-friendly corrosion inhibitors: Adsorption and inhibitive action of ethanol extracts of *Chomolaena odorata* L. For the corrosion of mild steel in H₂SO₄ solutions. *Int. J. Electrochem. Sci.* **2012**, *7*, 1997–2008.
60. Zakvi, S.; Mehta, G. Acid corrosion of mild steel and its inhibition by *Swertia angustifolia*-study by electrochemical techniques. *Trans. SAEST* **1988**, *23*, 407–410.
61. Faiz, M.; Zahari, A.; Awang, K.; Hussin, H. Corrosion inhibition on mild steel in 1 M HCl solution by *Cryptocarya nigra* extracts and three of its constituents (alkaloids). *RSC Adv.* **2020**, *10*, 6547–6562. [\[CrossRef\]](#)
62. Flick, E.W. *Corrosion Inhibitors: An Industrial Guide*; Noyes Publications: Park Ridge, NJ, USA, 1993.
63. Soltani, N.; Tavakkoli, N.; Khayat Kashani, M.; Jalali, M.R.; Mosavizade, A. Green approach to corrosion inhibition of 304 stainless steel in hydrochloric acid solution by the extract of *Salvia officinalis* leaves. *Corros. Sci.* **2012**, *62*, 122–135. [\[CrossRef\]](#)
64. Li, L.; Zhang, X.; Lei, J.; He, J.; Zhang, S.; Pan, F. Adsorption and corrosion inhibition of *Osmanthus fragrans* leaves extract on carbon steel. *Corros. Sci.* **2012**, *63*, 82–90. [\[CrossRef\]](#)
65. Faustin, M.; Maciuk, A.; Salvin, P.; Roos, C.; Lebrini, M. Corrosion inhibition of C38 steel by alkaloids extract of *Geissospermum laeve* in 1 M hydrochloric acid: Electrochemical and phytochemical studies. *Corros. Sci.* **2015**, *92*, 287–300. [\[CrossRef\]](#)